Modeling and Control for Dexterous Manipulation with a Personal Assistant Robot

Yang Qian [1, a], Ahmed Rahmani [2, b], Qian Chen [1, c], Songhua Shi [1, d], Fei Han [1, e]

[1] Shanghai Radio Equipment Research Institute, Shanghai, 200090, China,

[2] LAGIS, FRE CNRS 3303, Ecole Centrale de Lille, Villeneuve d'Ascq, 59650, France

[a]qianyang87@163.com, [b]ahmed.rahmani@ec-lille.fr, [c]qian_ch@163.com, [d]snake7946@sina.com, [e]mffthan@126.com

Abstract

This paper presents the modeling and control of a personal assistant robot manipulating an object. This robot is used for domestic tasks and can be regarded as a dual-arm/hand mobile manipulator system. First, the kinematics of the mobile platform part, the manipulator part, the dexterous hand part and the object is established by modified D-H method separately. Secondly, the kinematics of the mobile manipulator with hands is developed. The dynamics of the robot and the object is derived by Lagrange's theorem respectively. Then the constrained dynamics of the robot-object system is discussed. In order to make the object follow a desired trajectory, a control algorithm using computed torque method is proposed. This control method is based on the precise constrained dynamics. Finally, for simulation, the mobile manipulator system with the dexterous hands is developed using MATLAB. The simulation results have shown the efficiency of the proposed control method.

Keywords

Personal assistant robot; dexterous manipulation; dynamic modeling; computed torque control.

1. Introduction

In recent years, for creating a robot with dexterous manipulation, the study on control of powerful robots with dexterous arms has attracted significant attention. The project underway pursues the prototype development of a personal assistant robot for assistance tasks in household environments. It is a complex machine that consists of a mobile platform, two robotic arms and two dexterous hands. This type of robot is called a mobile manipulator [1-6]. So far there are many developed multi-fingered hands [7-13]. Although researches on mobile robots, robotic arms, manipulation by multi-fingered hands and even on mobile manipulators have been studied in various research institutes and universities, there are few works related to a redundant system considering mobile platform, arms and hands as a single system (as ARMAR-III [14] and Meka [15]). Most researches on robots have been developed in their own independent and separated lines without considering any coordination of each other. Object manipulation with a multi-fingered mobile manipulator is a challenging task, especially in service robot applications.

For control creation in mobile manipulation tasks, first, the kinematic and dynamic models of the dual-arm/hand mobile manipulator system should be developed. The kinematics involves determining the possible movements of the robot, without considering the forces and torques acting on the robot. Getting the kinematic model is the prerequisite needed to establish a dynamic model. The Denavit-Hartenberg representation [16], also called the D-H convention, describes a systematic way to develop the forward kinematics for rigid robots. This convention to develop reference frames is commonly used in robotic applications. There are two slightly different approaches to the convention: the so called standard D-H notation described in for example [17] and the Modified D-H form (MDH) found in [18].

The response to the forces and torques is the subject of the dynamics. There are several fundamental methods for the formulation of equations of motion, such as Newton-Euler formulation [19], Euler-Lagrange principle [20], Kane's method [21], and Screw theory [22]. All the above mentioned approaches have their own advantages and disadvantages when applied to complex robots like mobile manipulators. In this paper, MDH and the Euler-Lagrange methodology are chosen to lead our study.

Another important aspect of object manipulation is the control scheme implemented. The two main types of control are force control and position control. The execution of object manipulation requires controlling the interaction forces to ensure grasp stability. This is accomplished by satisfying form or force closure conditions. In this paper, Linear Matrix Inequalities (LMI) is used to optimize the grasping forces [23, 24]. On condition that the precise dynamic model of the robot–object system has been obtained, many classical dynamic model based trajectory tracking methods such as computed torque method and feedforward control law can be applied for the position control. In this paper a control scheme for the robot-object system intended for the study of dexterous manipulation is proposed by the computed torque method.

The rest of this paper is organized as follows. In Section 2, the kinematic models of the mobile platform part, the manipulator part, the dexterous hand part and the object are established separately. Then the kinematics of the mobile manipulator with hands is developed. In Section 3, the dynamics of the robot and the object is derived by Lagrange's theorem respectively. In Section 4, the constrained dynamics of the robot-object system is discussed. Section 5 proposes a model based control method in order to track a desired trajectory imposed to the object. Numerical simulation results are shown in Section 6 to illustrate the effectiveness of the proposed control method. Finally, Section 7 concludes the paper.

2. Kinematic Modeling

In this section, the overall kinematic equations of the robot are discussed briefly. The service robot is built from a set of links, joined with revolute joints that can rotate the robot around a given axis. If the dexterous hands are not taken into account, the robot's links and joints can be divided into five main parts: mobile platform, waist, left arm, right arm and head. As shown in Figure 1(a), three kinematic loops are formulated:

- Loop a: it contains platform, waist, right shoulder and right arm.
- Loop b: it contains platform, waist, left shoulder and left arm.
- Loop c: it contains platform, waist, neck and head.

Substituting a pair of dexterous hands for the end-effectors, the complete robot can be divided into nine kinematic loops Loop R1, Loop R2, Loop R3, Loop R4, Loop L1, Loop L2, Loop L3, Loop L4 and Loop c as denoted in Figure 1(b). Figure 1 (b) shows that each independent loop contains a finger.

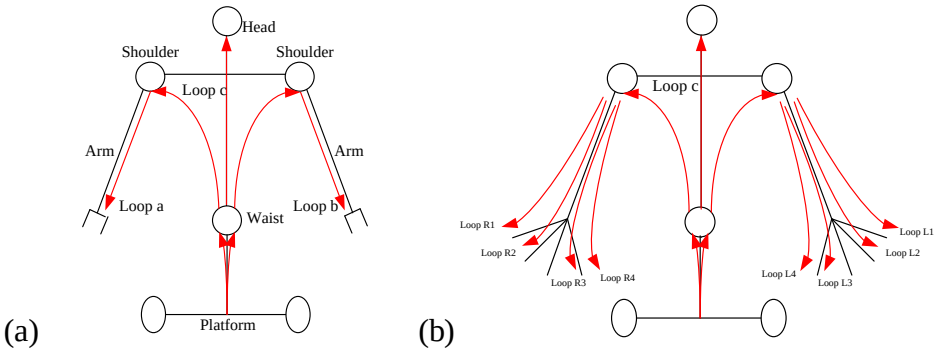

Figure 1: Kinematic loops (a) The simplified kinematic loops of the robot without fingers (b) The simplified kinematic loops of the robot with fingers

As can be seen, the personal assistant robot has a tree-like structure with multi-DOF (degree of freedom), and each finger can be treated as a branch on this tree. The complete kinematic model of the multi-fingered mobile manipulator can be obtained by modeling these separate loops. Due to the

independence the kinematic models of all the loops can be derived by the same approach. Note that, in the following sections, Loop c will be neglected and not be simulated because it just supports the vision system.

In this paper, q denotes the vector of generalized coordinates of Loop a and Loop b and may be separated into four sets $q = \begin{bmatrix} q_v^T & q_w^T & q_r^T & q_l^T \end{bmatrix}^T \in \Re^p$. The subscripts v, w, r and l represent the mobile platform, waist, right arm and left arm respectively. $q_v \in \Re^m$ describes the vector of generalized coordinates of the mobile platform, $q_w \in \Re^n$ is the vector of generalized coordinates of the waist, and $q_r, q_l \in \Re^a$ are the vectors of generalized coordinates of the right and left arms respectively. The total number of the generalized coordinates p is $m+n+2a$. The vector of generalized coordinates q' of Loop R1, R2, R3, R4, L1, L2, L3 and L4 may be divided into three sets $q' = \begin{bmatrix} q_v^T & q_b^T & q_f^T \end{bmatrix} \in \Re^{p'}$. The subscripts v, b, f denote the mobile platform, robot body (including waist and dual arms) and fingers respectively. $q_b = \begin{bmatrix} q_w^T & q_r^T & q_l^T \end{bmatrix}^T \in \Re^{n+2a}$ describes the vector of generalized coordinates of the waist and two arms, $q_f = \begin{bmatrix} q_{rf}^T & q_{lf}^T \end{bmatrix}^T$, $q_{rf}, q_{lf} \in \Re^b$, are the vectors of generalized coordinates of the right and left hands and the total number of the generalized coordinates $p' = m+n+2a+2b$.

In this section, first, the mobile platform, the manipulator parts and the dexterous hands are discussed separately. Then the kinematics of Loop R1, R2, R3, R4, L1, L2, L3 and L4 are derived using a similar method. Finally, the kinematics of a rigid body is discussed.

2.1 Mathematical Model of Differential Wheeled Platform

The platform has two driving wheels (conventional wheels) and two passive supporting wheels (omni wheels). The two driving wheels are independently driven by the DC motors. The schematic of this differential wheeled robot is shown in Figure 2.

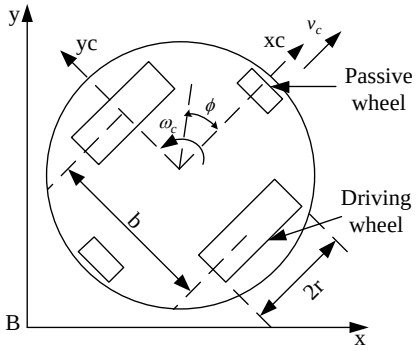

Figure 2: Schematic of differential wheeled robot

b : the distance between the driving wheels;

r : the radius of each driving wheel.

The nonholonomic constraint states that the robot can only move in the direction normal to the axis of the driving wheels, i.e., the mobile base satisfies the conditions of pure rolling and non slipping [25]:

$$\dot{y}_c \cos\phi - \dot{x}_c \sin\phi = 0 \tag{1}$$

where $\begin{bmatrix} x_c & y_c \end{bmatrix}^T$ are the coordinates of the center of mass in the world coordinate system, and ϕ is the heading angle of the platform measured from the x-axis of the world coordinate system.

Let the Lagrange coordinates of the mobile platform be $q_v = \begin{bmatrix} x_c & y_c & \phi \end{bmatrix}^T$ which represent the position of the robot in the world coordinate system, the constraint can be written in the form:

$$A_v(q_v)\dot{q}_v = 0 \tag{2}$$

which is according to (1), where $A_v(q_v) = \begin{bmatrix} -\sin\phi & \cos\phi & 0 \end{bmatrix}$.

2.2 Forward Kinematics of Manipulator

As mentioned above, without the dexterous hands, the robot can be divided into three independent loops. For the body (excluding mobile platform), each loop is considered as a linkage, which is defined to be a set of attached rigid bodies. Let us take Loop a as an example. Each rigid body is referred to as a link, denoted by W. Let W_1, W_2, . . ., and W_{n+a} denote a set of n+a links. The kinematic analysis mainly includes two sides, one is the forward kinematic analysis, and the other is the inverse kinematic (IK) analysis. The forward kinematic analysis means that the location and pose of the linkage end point in a given reference coordinate system can be worked out with the given geometry parameters of the links and the variables of the joints. Let $Q=\begin{bmatrix} q_w^T & q_r^T \end{bmatrix}^T=\begin{bmatrix} q_1 & q_2 & \dots & q_{n+a} \end{bmatrix}^T$ denote the set of angles of rotational joints, then Q yields an acceptable position and orientation of the links in the chain by using the homogeneous transformation matrix. Given the matrix ${}^{i-1}T_i$ expressing the difference between the coordinate frame of W_{i-1} and the coordinate frame of W_i, the application of ${}^{i-1}T_i$ transforms any point in W_{i-1} to the body frame of W_i. Repeating the above procedure, the end-effector location $\begin{bmatrix} x' & y' & z' \end{bmatrix}^T$ in the frame $\sum_0$ attached to the mobile base is determined by multiplying the transformation matrices and the end-effector location $\begin{bmatrix} x & y & z \end{bmatrix}^T \in W_{n+a}$:

$$\begin{bmatrix} x' & y' & z' & 1 \end{bmatrix}^T = {}^0T_1\,{}^1T_2 \dots {}^{n+a-1}T_{n+a} \begin{bmatrix} x & y & z & 1 \end{bmatrix}^T = T \begin{bmatrix} x & y & z & 1 \end{bmatrix}^T \tag{3}$$

where

$$T=\begin{bmatrix} {}^0R_{n+a} & {}^0P_{n+a} \\ 0\dots0 & 1 \end{bmatrix}=\begin{bmatrix} n_x & o_x & a_x & p_x \\ n_y & o_y & a_y & p_y \\ n_z & o_z & a_z & p_z \\ 0 & 0 & 0 & 1 \end{bmatrix} \in \Re^{4\times4},\ {}^0R_{n+a}=\begin{bmatrix} n_x & o_x & a_x \\ n_y & o_y & a_y \\ n_z & o_z & a_z \end{bmatrix} \in \Re^{3\times3} \text{ and } {}^0P_{n+a}=\begin{bmatrix} p_x & p_y & p_z \end{bmatrix}^T \in \Re^3 \text{ give}$$

the rotation axis and the position in the frame $\sum_0$, respectively.

The above formula represents the forward kinematics for positioning a linkage by a specific joint configuration. The MDH method is used to analyze the kinematics. Figure 3 shows the Modified form of Denavit-Hartenberg. Frame i has its origin along the axis of joint i.

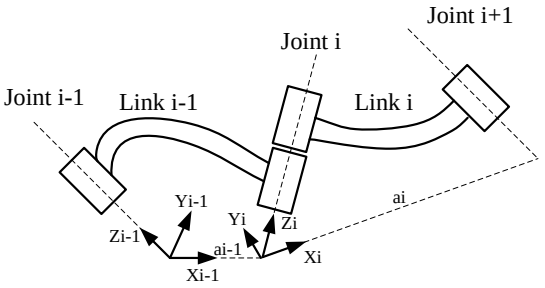

Figure 3: Modified form of Denavit-Hartenberg

According to Modified form of Denavit-Hartenberg, the transformation matrix could be expressed by the following equation:

$$\begin{aligned} {}^{i-1}T_i &= Rot(x,\alpha_{i-1}) \times Trans(x,a_{i-1}) \times Rot(z,q_i) \times Trans(z,d_i) \\ {}^{i-1}T_i &= \begin{bmatrix} \cos q_i & -\sin q_i & 0 & a_{i-1} \\ \sin q_i \cos\alpha_{i-1} & \cos q_i \cos\alpha_{i-1} & -\sin\alpha_{i-1} & -d_i \sin\alpha_{i-1} \\ \sin q_i \sin\alpha_{i-1} & \cos q_i \sin\alpha_{i-1} & \cos\alpha_{i-1} & d_i \cos\alpha_{i-1} \\ 0 & 0 & 0 & 1 \end{bmatrix} \end{aligned} \tag{4}$$

where

α_{i-1} = the angle between Z_{i-1} and Z_i measured about X_{i-1},
a_{i-1} = the distance from Z_{i-1} to Z_i measured along X_{i-1},
q_i = the angle between X_{i-1} and X_i measured about Z_i,
d_i = the distance from X_{i-1} to X_i measured along Z_i.

Figure 4 illustrates the idea of attaching frames of the mobile manipulator according to MDH. The frame $x_0 y_0 z_0$ is attached to the mobile base. And the other frames are attached to each of the links.

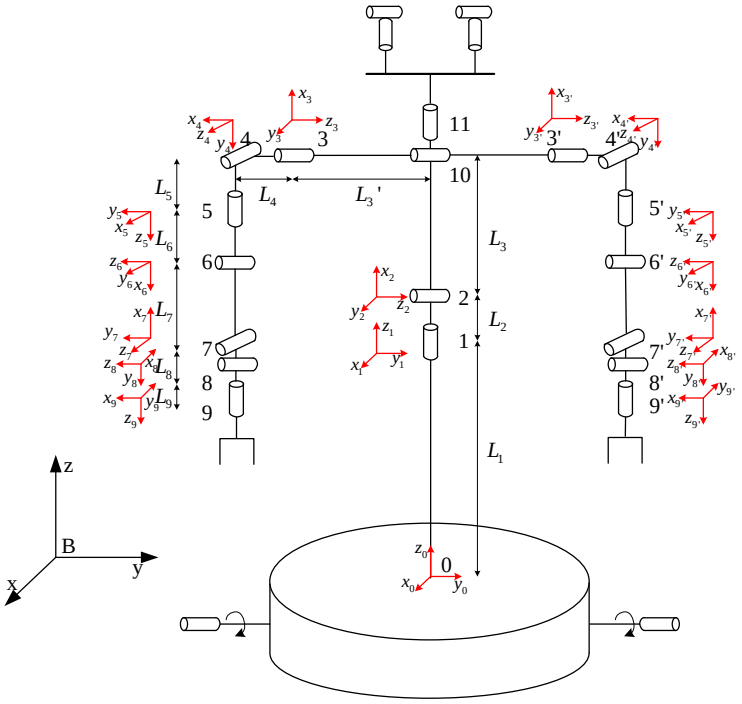

Figure 4: Coordinate frames attached to mobile manipulator

MDH parameters of all joints are depicted in Table 1.

Table 1: MDH parameters of mobile base and manipulators

#	α	a	q	d
0-1	0 °	0	0 °	$L_1 + L_2$
1-2	-90 °	0	-90 °	0
2-3	0 °	L_3	0 °	$-(L_3' + L_4)$
2-3’	0 °	L_3	0 °	$(L_3' + L_4)$
3-4/3’-4’	-90 °	0	90 °	0
4-5/4’-5’	-90 °	0	-90 °	$L_5 + L_6$
5-6/5’-6’	-90 °	0	-90 °	0
6-7/6’-7’	-90 °	L_7	180 °	0
7-8/7’-8’	-90 °	$-L_8$	90 °	0
8-9/8’-9’	-90 °	0	-90 °	0

Tasks to be performed by a manipulator are in task space, whereas actuators work in joint space. Task space includes orientation matrix and position vector. However, joint space is represented by joint angles. The conversion from the position and orientation of the end-effector in task space to the joint angles in joint space is called as IK problem. The inverse formula of (3) forms IK problem in which a set of joint angles need to be calculated corresponding to a given spatial constraint of the end-effector. In this paper the numbers of joint DOFs of all loops are more than the number of spatial constraints, the system is redundant and there are multiple solutions.

2.3 Kinematics Analysis of Dexterous Hand

This part sets out the framework for the mathematical modeling of kinematic equations for the multi-fingered hand. Forward kinematics is used to obtain the fingertip position and orientation according to the finger joint angles.

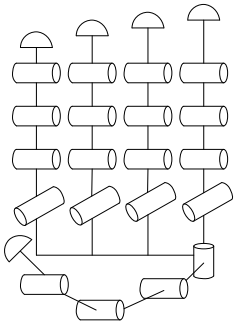

Figure 5: Structure of dexterous hand

According to the mechanical structure, each dexterous hand is composed of five fingers and all of the fingers have the same size and shape. Among these five fingers, the last two fingers (the ring and the little fingers) are mechanically coupled so that they keep the same motion. Therefore these two fingers just have 4 DOFs and the little finger only plays a supportive role. Thus, this hand totally has 16 DOFs. The kinematic structure of the finger mechanism is based on a simplification of a human finger. In this paper the last two fingers are considered as one finger.

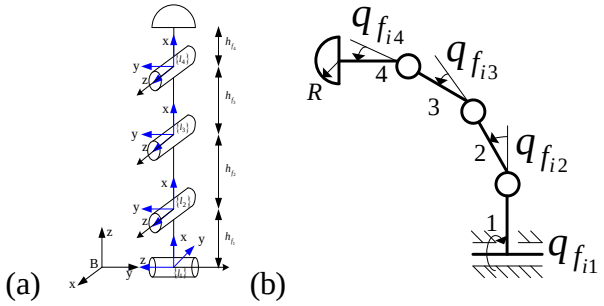

Figure 6: Finger linage (a) Definition of reference frames (b) Geometry of a finger module

As indicated in Figure 6, the mechanism consists of four joints. The angular positions of the first and second joints of finger i of the right (left) hand are defined by $q_{r(l)f_{i1}}$ and $q_{r(l)f_{i2}}$. The angular positions of the third and fourth joints are defined by $q_{r(l)f_{i4}}$ and $q_{r(l)f_{i4}}$, respectively. Neglecting the superscripts r and l, $q_{f_i} = \begin{bmatrix} q_{f_{i1}} & q_{f_{i2}} & q_{f_{i3}} & q_{f_{i4}} \end{bmatrix}^T$ represents the generalized coordinates of each finger. Table 2 shows the dimensions of the fingers.

Table 2: Kinematic parameters of fingers

Link lengths (mm)		Location of center of mass (mm)	
h_{f_1}	21.00	1	5
h_{f_2}	28.53	2	20

h_{f_3}	27.16	3	20
h_{f_4}	18.50	4	7.5

Considering the fingertip as the end point, the forward kinematics of the finger is also derived by MDH method. The parameters of all joints are depicted in Table 3.

Table 3: MDH parameters of fingers

#	α	a	q	d
0-1	90 °	0	90 °	0
1-2	90 °	h_{f_1}	0 °	0
2-3	0 °	h_{f_2}	0 °	0
3-4	0 °	h_{f_3}	0 °	0

2.4 Robot Kinematics with Dexterous Hands

Consider a bimanual manipulation system composed by a mobile platform, a two s waist and a dual-arm/hand system. The direct kinematics can be computed by introducing a frame $\sum_B$ fixed with the ground, a frame, $\sum_0$, attached at the center of the mobile base, two frames, $\sum_r$ and $\sum_l$, attached at the bases of the right and left arms, respectively, and two frames, $\sum_{rp}$ and $\sum_{lp}$, attached to the palms of the right and left hands, respectively. Moreover, assuming that each arm ends with a robotic hand composed by N fingers, it is useful to introduce a frame $\sum_{rf_i}$ ($\sum_{lf_i}$), attached to the distal phalanx of finger i ($i = 1 \ldots N$) of the right (left) hand.

Consider Loop R_i. The pose of $\sum_{rf_i}$ with respect to the base frame $\sum_B$ can be represented by the well known (4×4) homogeneous transformation matrix ${}^B T_{rf_i}$ (${}^B R_{rf_i}$, ${}^B P_{rf_i}$), where ${}^B R_{rf_i}$ is the (3×3) rotation matrix expressing the orientation of $\sum_{rf_i}$ with respect to the frame $\sum_B$ and ${}^B P_{rf_i}$ is the (3×1) position vector of the origin of $\sum_{rf_i}$ with respect to $\sum_B$.

Hence, the direct kinematics can be expressed as:

$$ {}^B T_{rf_i} = {}^B T_0 \, {}^0 T_r \, {}^r T_{rp} \, {}^{rp} T_{rf_i} \tag{5} $$

where ${}^B T_0$ is the matrix relating the mobile base frame to the base frame, ${}^0 T_r$ is the matrix at the basis of the right arm to the mobile base frame and depends on the waist joint vector, ${}^r T_{rp}$ is the matrix relating the right palm frame to the base frame of the right arm and depends on the joint vector of the right arm, and ${}^{rp} T_{rf_i}$ is the matrix relating the frame attached to the distal phalanx of finger i to the palm frame of the right hand and depends on the finger joint vector q_{rf_i}, where the fingers are assumed to be identical. An equation similar to (5) holds for the left hand fingers (Loop L_i), with subscript l in place of subscript r.

Due to the branched structure of the mobile manipulator, the motions of both the right and left arms are independent. Therefore, the kinematics of the right and left hands can be considered separately. Hence, in the sequel, the superscripts r and l will be omitted and will be used explicitly only when it is required to distinguish between the right and the left arm.

The differential kinematic equation relating the joint velocities to the velocity of finger frame $\sum_{f_i}$ can be written as:

$$ V_{f_i} = J_{f_i} \dot{q}_i ' \tag{6} $$

where $q_i' = \begin{bmatrix} q_v^T & q_b^T & q_{f_i}^T \end{bmatrix}^T$ and J_{f_i} is the Jacobian matrix of the mobile part, the waist, the arm, ending with the i_{th} finger.

Therefore, the differential kinematic equation of the complete mobile base-waist-arm-hand system can be written in the form:

$$V_f = J_f \dot{q}' \tag{7}$$

where $V_f = \begin{bmatrix} V_{f_1}^T & \cdots & V_{f_N}^T \end{bmatrix}^T$, $q' = \begin{bmatrix} q_v^T & q_b^T & q_{f_1}^T & \cdots & q_{f_N}^T \end{bmatrix}^T$ and J_f is the Jacobian matrix of the overall mobile base-waist-arm-hand system.

2.5 Kinematic Description of Object

A rigid body that is free to move in space has six DOFs. This can be described by an open kinematic chain with six joints (three prismatic joints and three revolute joints). To describe the posture of the body we consider ZYZ Euler rotation. Similar to the previous case it is easy to obtain the direct kinematics. The homogeneous matrix which describes the posture of the object (O) in space relative to the fixed reference frame Σ_B depends on the values of the local parameterization $X_o = \begin{bmatrix} x & y & z & \alpha & \beta & \gamma \end{bmatrix}^T$. ${}^B P_o = \begin{bmatrix} x & y & z \end{bmatrix}^T \in \Re^3$ is the object position relative to Σ_B and $\begin{bmatrix} \alpha & \beta & \gamma \end{bmatrix}^T$ represents the ZYZ angles. The rotation axis of the object in the frame Σ_B is denoted by ${}^B R_o$ which is expressed as following:

$$\begin{aligned} {}^B R_o &= Rot(z,\alpha) Rot(y,\beta) Rot(z,\gamma) \\ &= \begin{bmatrix} \cos\alpha & -\sin\alpha & 0 \\ \sin\alpha & \cos\alpha & 0 \\ 0 & 0 & 1 \end{bmatrix} \begin{bmatrix} \cos\beta & 0 & \sin\beta \\ 0 & 1 & 0 \\ -\sin\beta & 0 & \cos\beta \end{bmatrix} \begin{bmatrix} \cos\gamma & -\sin\gamma & 0 \\ \sin\gamma & \cos\gamma & 0 \\ 0 & 0 & 1 \end{bmatrix} \end{aligned} \tag{8}$$

3. Dynamic Modeling

3.1 Dynamic Modeling of Mobile Manipulator

The dynamics of mobile manipulators subject to kinematic constraints can be obtained using the Lagrangian approach in the form [26]:

$$M(q)\ddot{q} + C(q,\dot{q})\dot{q} + F(q) + A^T(q)\lambda + \tau_d = E(q)\tau \tag{9}$$

where r kinematic constraints are described by:

$$A(q)\dot{q} = 0, \tag{10}$$

and $q \in \Re^p$ denotes the p generalized coordinates, $M(q) \in \Re^{p \times p}$ is a symmetric and positive definite inertia matrix, $C(q,\dot{q}) \in \Re^{p \times p}$ presents a centripetal and Coriolis matrix, $F(q,\dot{q}) \in \Re^p$ is a friction and gravity vector, $A(q) \in \Re^{r \times p}$ represents a constraint matrix, $\lambda \in \Re^r$ is the Lagrange multiplier vector which denotes the constraint forces, $\tau_d \in \Re^p$ denotes unknown bounded disturbances including unstructured dynamics, $E(q) \in \Re^{p \times (p-r)}$ is the input transformation matrix, and $\tau \in \Re^{p-r}$ is a torque input vector.

According to the standard matrix theory, there exists a full rank matrix $S(q) \in \Re^{p \times (p-r)}$ formed by $p-r$ columns that span the null space of $A(q)$ defined in (10). i.e..

$$S^T(q)A^T(q) = 0 \tag{11}$$

As mentioned above, the generalized coordinate q of Loop a and Loop b is separated into four sets $q = \begin{bmatrix} q_v^T & q_w^T & q_r^T & q_l^T \end{bmatrix}^T$. We can find an auxiliary vector $\zeta = \begin{bmatrix} v^T & \dot{q}_w^T & \dot{q}_r^T & \dot{q}_l^T \end{bmatrix}^T \in \Re^{(p-r)}$ such that for all t,

$$\dot{q} = S(q)\zeta \text{ or } \dot{q}_v = S_v(q)v \tag{12}$$

v can be defined as $\begin{bmatrix}\dot{\theta}_r & \dot{\theta}_l\end{bmatrix}^T$ or $[v_c \quad \omega_c]^T$, where $\dot{\theta}_r$ and $\dot{\theta}_l$ are the angular velocities of the right and left wheels, respectively; v_c and ω_c are the linear and angular velocities of the mobile base, respectively.

The time derivate of (12) is:

$$\ddot{q} = S(q)\dot{\zeta}(t) + \dot{S}(q)\zeta(t) \tag{13}$$

Multiplying both sides of (9) by S^T and rewriting it as:

$$\bar{M}\dot{\zeta} + \bar{C}\zeta + \bar{F} + \bar{\tau}_d = \bar{E}\tau \tag{14}$$

where $\bar{M} = S^T MS, \bar{C} = S^T CS + S^T M\dot{S}, \bar{F} = S^T F, \bar{\tau}_d = S^T \tau_d$, and $\bar{E} = S^T E$.

Property 1: The inertia matrix $\bar{M}(q)$ is symmetric and positive definite.

Property 2: Matrix $\dot{\bar{M}}(q) - 2\bar{C}(q,\dot{q})$ is skew-symmetric.

Property 3: The time-varying unstructured disturbance term τ_d is bounded by $\sup_t \| \tau_d \| \leq \tau_N$.

Using the separated generalized coordinates $q = \begin{bmatrix} q_v^T & q_w^T & q_r^T & q_l^T \end{bmatrix}^T$, (9) can be expressed as:

$$\begin{bmatrix} M_v & M_{vw} & M_{vr} & M_{vl} \\ M_{wv} & M_w & M_{wr} & M_{wl} \\ M_{rv} & M_{rw} & M_r & 0 \\ M_{lv} & M_{lw} & 0 & M_l \end{bmatrix} \begin{bmatrix} \ddot{q}_v \\ \ddot{q}_w \\ \ddot{q}_r \\ \ddot{q}_l \end{bmatrix} + \begin{bmatrix} C_v & C_{vw} & C_{vr} & C_{vl} \\ C_{wv} & C_w & C_{wr} & C_{wl} \\ C_{rv} & C_{rw} & C_r & 0 \\ C_{lv} & C_{lw} & 0 & C_l \end{bmatrix} \begin{bmatrix} \dot{q}_v \\ \dot{q}_w \\ \dot{q}_r \\ \dot{q}_l \end{bmatrix}$$
$$+ \begin{bmatrix} F_v \\ F_w \\ F_r \\ F_l \end{bmatrix} + \begin{bmatrix} A_v^T(q_v)\lambda \\ 0 \\ 0 \\ 0 \end{bmatrix} + \begin{bmatrix} \tau_{dv} \\ \tau_{dw} \\ \tau_{dr} \\ \tau_{dl} \end{bmatrix} = \begin{bmatrix} E_v\tau_v \\ \tau_w \\ \tau_r \\ \tau_l \end{bmatrix} \tag{15}$$

Equations (9) and (15) represent the dynamic equations of the mobile manipulator subject to kinematic constraints without the dexterous hands.

3.2 Dynamic Modeling of Mobile Manipulator with Hands

The dexterous hands can be mounted on the ends of the robotic arms directly. Based on the discussion given above, the complete dynamic model with a pair of dexterous hands can be expressed as:

$$\begin{bmatrix} M_v & M_{vb} & M_{vf} \\ M_{bv} & M_b & M_{bf} \\ M_{fv} & M_{fb} & M_f \end{bmatrix} \begin{bmatrix} \ddot{q}_v \\ \ddot{q}_b \\ \ddot{q}_f \end{bmatrix} + \begin{bmatrix} C_v & C_{vb} & C_{vf} \\ C_{bv} & C_b & C_{bf} \\ C_{fv} & C_{fb} & C_f \end{bmatrix} \begin{bmatrix} \dot{q}_v \\ \dot{q}_b \\ \dot{q}_f \end{bmatrix} + \begin{bmatrix} F_v \\ F_b \\ F_f \end{bmatrix}$$
$$+ \begin{bmatrix} A_v^T(q_v)\lambda \\ 0 \\ 0 \end{bmatrix} + \begin{bmatrix} \tau_{dv} \\ \tau_{db} \\ \tau_{df} \end{bmatrix} = \begin{bmatrix} E_v\tau_v \\ \tau_b \\ \tau_f \end{bmatrix} \tag{16}$$

Considering the nonholonomic constraints and their time-derivatives, the dynamics can be expressed as:

$$\begin{bmatrix} S_v^T M_v S_v & S_v^T M_{vb} & S_v^T M_{vf} \\ M_{bv} S_v & M_b & M_{bf} \\ M_{fv} S_v & M_{fb} & M_f \end{bmatrix} \begin{bmatrix} \dot{v} \\ \ddot{q}_b \\ \ddot{q}_f \end{bmatrix} + \begin{bmatrix} S_v^T M_v \dot{S}_v + S_v^T C_v S_v & S_v^T C_{vb} & S_v^T C_{vf} \\ M_{bv}\dot{S}_v + C_{bv} S_v & C_b & C_{bf} \\ M_{fv}\dot{S}_v + C_{fv} S_v & C_{fb} & C_f \end{bmatrix} \begin{bmatrix} v \\ \dot{q}_b \\ \dot{q}_f \end{bmatrix}$$
$$+ \begin{bmatrix} S_v^T F_v \\ F_b \\ F_f \end{bmatrix} + \begin{bmatrix} S_v^T \tau_{dv} \\ \tau_{db} \\ \tau_{df} \end{bmatrix} = \begin{bmatrix} S_v^T E_v \tau_v \\ \tau_b \\ \tau_f \end{bmatrix} \tag{17}$$

where the subscripts v, b, f denote the mobile platform, the body including the waist and the arms, and the fingers respectively.

Similarly, the complete dynamic equation can also be described in a compact form:

$$\bar{M}'\dot{\xi}+\bar{C}'\xi+\bar{F}'+\bar{\tau}_d'=\bar{E}'\tau' \tag{18}$$

where

$$\bar{M}'=\begin{bmatrix} S_v^T M_v S_v & S_v^T M_{vb} & S_v^T M_{vf} \\ M_{bv}S_v & M_b & M_{bf} \\ M_{fv}S_v & M_{fb} & M_f \end{bmatrix}, \bar{C}'=\begin{bmatrix} S_v^T M_v \dot{S}_v + S_v^T C_v S_v & S_v^T C_{vb} & S_v^T C_{vf} \\ M_{bv}\dot{S}_v + C_{bv}S_v & C_b & C_{bf} \\ M_{fv}\dot{S}_v + C_{fv}S_v & C_{fb} & C_f \end{bmatrix},$$

$$\bar{F}'=\begin{bmatrix} S_v^T F_v \\ F_b \\ F_f \end{bmatrix}, \bar{\tau}_d'=\begin{bmatrix} S_v^T \tau_{dv} \\ \tau_{db} \\ \tau_{df} \end{bmatrix}, \bar{E}'\tau'=\begin{bmatrix} S_v^T E_v \tau_v \\ \tau_b \\ \tau_f \end{bmatrix}, \xi=\begin{bmatrix} v \\ \dot{q}_b \\ \dot{q}_f \end{bmatrix}.$$

3.3 Object Dynamics

As mentioned above, a rigid body with six DOFs can be described by a kinematic chain with six open link, three revolute and three prismatic joints. Thus, the dynamic equations can be obtained in a similar manner:

$$M_o(X_o)\ddot{X}_o + C_o(X_o,\dot{X}_o)\dot{X}_o + N_o(X_o,\dot{X}_o) = F_o \tag{19}$$

where $X_o=[x \quad y \quad z \quad \alpha \quad \beta \quad \gamma]^T$ represents the posture of the object relative to the fixed reference, while F_o is the wrench applied to the center of mass of the object; the dynamic matrices $M_o \in \Re^{6\times6}, C_o \in \Re^{6\times6}$ and $N_o \in \Re^{6\times1}$ are the acceleration-related inertia matrix, Coriolis and centrifugal matrix and vector of friction and gravity respectively.

4. Robot-Object System

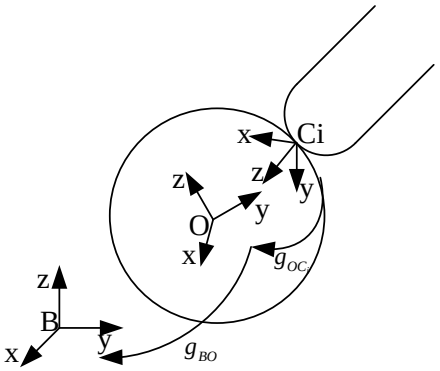

Figure 7: Coordinate frames and representation of a finger touching a sphere

Consider an object manipulated by a robotic hand as a closed kinematic chain. We assume that the contact locations are fixed on the object. First, we introduce the reference frames at the contact point. Figure 7 shows a situation where there is a contact from a finger with the coordinate frame Σ_{C_i}. Frame Σ_B is fixed with the ground. Σ_O denotes the object coordinate frame. The choice of reference point is always the center of mass of the object.

For clarity from now on we will consider two reference frames at the contact point: one is on the object ($\Sigma_{C_{O_i}}$) and the other one is on the fingertip ($\Sigma_{C_{fi}}$). The position and orientation of the contact point on the object with respect to the reference system centered on the object (Σ_O) are described by the homogeneous matrix g_{OC_i}, which depends on the local coordinates of this point. The posture of the object relative to the reference frame Σ_B is expressed by the homogeneous matrix g_{BO}. Note that in

this section homogeneous transformation matrix is denoted by g in order to distinguish between homogeneous matrix and torsion T_f which will be discussed later.

4.1 Constraint on Contact Force

(a) Wrenches between the fingers and the grasped object

A contact is basically a mapping between the wrench exerted by a finger at the contact point and the resultant wrench at a reference point on an object. There are many different contact types used to describe the wrench a finger is exerting on an object. They are frictionless point contact, point contact with friction, and soft-finger contact. In this section, we study hard-finger contact model which belongs to the second type. The hard-finger contact allows the forces to be applied within the friction cone. For the i_{th} finger, this is represented by:

$$F_{ci} = B_{ci} f_{ci}, f_{ci} \in FC_{ci} \tag{20}$$

where the forces applied by a contact are modeled as a wrench F_{ci} applied at the origin of the contact frame ($\Sigma_{C_{O_i}}$ or $\Sigma_{C_{fi}}$) ; f_{ci} is a vector represents the magnitude of the contact forces applied by the finger; B_{ci} is wrench basis matrix and for the hard-finger contact it is defined as: $B_{ci} = \begin{bmatrix} 1 & 0 & 0 & 0 & 0 & 0 \\ 0 & 1 & 0 & 0 & 0 & 0 \\ 0 & 0 & 1 & 0 & 0 & 0 \end{bmatrix}^T$.

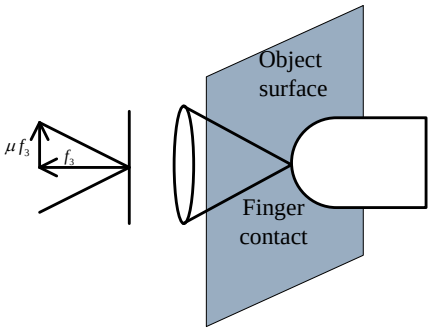

Figure 8: Hard-finger contact model

The set FC_{ci} represents the friction cone of contact i, and the hard-finger model applies:

$$FC_{c_i} = \{ f_{c_i} \in \Re^3 : \frac{1}{\mu_i} \sqrt{f_{i1}^2 + f_{i2}^2} \le f_{i3}, f_{i3} \ge 0 \} \tag{21}$$

where $f_{ci} = [\, f_{i1} \quad f_{i2} \quad f_{i3} \,]^T$, f_{i1} and f_{i2} denote the tangent components of the friction force, f_{i3} denotes the normal component of the contact force, and μ_i denotes the friction coefficient.

(b) Grasp map

Grasp map is used to determine the effect of contact wrenches on the object. To determine the effect, the wrenches must be transformed to the object coordinate frame. If $(R_{oc_{fi}}, p_{oc_{fi}})$ is the configuration of the i_{th} contact frame relative to the object frame, then the wrench exerted by this contact can be written in the object coordinate frame as:

$$F_o = Ad_{goc_{fi}}^{-T} F_{ci} = Ad_{goc_{fi}}^{-T} B_{ci} f_{ci} \tag{22}$$

where $Ad_{goc_{fi}}^{-T}$ is the wrench transformation matrix that maps contact wrench to object wrench.

We define the grasp matrix G_i as a linear map between the contact forces and the wrench act on the object of finger i:

$$G_i = Ad_{goc_{fi}}^{-T} B_{ci} \tag{23}$$

If we consider N fingers in contact, the total wrench is the combination of all wrenches on the object due to the fingers. The grasp matrix G that maps all contact forces on the object is:

$$G = \begin{bmatrix} G_1 & \dots & G_N \end{bmatrix} = \begin{bmatrix} Ad_{goc_{f1}}^{-T} B_{c1} & \dots & Ad_{goc_{fN}}^{-T} B_{cN} \end{bmatrix} \tag{24}$$

In this way the total wrench on the object is given by:

$$F_o = Gf_c \tag{25}$$

where $f_c = \begin{bmatrix} f_{c1}^T & f_{c2}^T & \cdots & f_{cN}^T \end{bmatrix}^T$.

(c) Force-closure

If a grasp can resist any applied wrench, the grasp is said to be force-closure. When grasping an object and lifting it from the table, it is necessary to apply appropriate wrenches at appropriate locations on the object so as not to allow gravity or possibly other external forces to pull the object out of the grasp. If a grasp can resist any external wrench F_e applied to the object, there exist contact forces $f_c \in FC_c$, such that:

$$Gf_c = -F_e \tag{26}$$

(d) Internal force

A key feature of a force-closure grasp is the existence of internal forces. Internal force is a set of contact forces which result in no net force on the object.

$$F_N \in N(G), GF_N = 0 \tag{27}$$

Internal forces can be used to insure that the contact forces satisfy the friction cone constraints.

4.2 Grasp Constraints

In this case, the constraints between the object and the fingers can be formulated by requiring that certain velocities are equal. For example, at a given contact point, the velocity of the contact point on the fingertip and that on the object must agree in the direction normal to the surface.

(a) Grasp constraints of multi-fingered hand

Recall that for the hand each finger is as an open kinematic chain, the spatial velocity of the fingertip can be written as:

$$V_{s_i f_i}^{f_i} = J_{s_i f_i}^{f_i}(q_{f_i}) \dot{q}_{f_i} \tag{28}$$

where $J_{s_i f_i}^{f_i}(q_{f_i})$ is the distal Jacobian matrix that transforms the angular velocities ($\dot{q}_{f_i}$) of finger joints to the velocity of end of a finger($V_{s_i f_i}^{f_i}$) in the frame attached to the finger's end ; Σ_{s_i} is the base frame of the i_{th} finger attached to the palm and at the point where this finger is connected.

Assume that each finger has a fingertip with known shape. The transformation $g_{f_i c_{f_i}}$ from the end of the finger to the contact point at the i_{th} fingertip depends on the local coordinates of the contact point on the surface of the fingertip.

In general, the directions in which the motions are constrained are precisely those in which the forces can be exerted. Hence, for a contact with the wrench basis B_{c_i} which has been illustrated in equation (20), we require that:

$$B_{c_i}^T V_{c_{oi} c_{f_i}}^{c_{f_i}} = 0 \tag{29}$$

The explicit form of the relative velocity between the fingertip and the object at the contact point is:

$$V_{c_{oi} c_{f_i}}^{c_{f_i}} = Ad_{g_{c_{f_i} f_i}} J_{s_i f_i}^{f_i} \dot{q}_{f_i} - Ad_{g_{c_{f_i} o}} V_{po}^{o} \tag{30}$$

where V_{po}^{o} is the velocity of the object relative to the palm in the object frame, and $g_{c_{f_i} o}$ represents the homogeneous transformation matrix from the object frame Σ_O to the contact frame $\Sigma_{C_{f_i}}$ on the fingertip, which is as:

$$g_{c_{f_i} o} = g_{c_{f_i} c_{oi}} g_{c_{oi} o} \tag{31}$$

where $g_{c_{fi}c_{oi}}$ represents the homogeneous transformation from the frame $\sum_{C_{O_i}}$ to the frame $\sum_{C_{fi}}$ and $g_{c_{oi}o}$ represents the homogeneous transformation matrix from the object frame $\sum_O$ to the contact frame $\sum_{C_{O_i}}$ on the object.

Then

$$B_{c_i}^T Ad_{g_{c_{fi}f_i}} J_{s_i f_i}^{f_i} \dot{q}_{f_i} = B_{c_i}^T Ad_{g_{c_{fi}o}} V_{po}^o \tag{32}$$

Using (23) and (24), for the hand with N fingers, the contact kinematics has the form:

$$J_h(q_f)\dot{q}_f = G^T V_{po}^o \tag{33}$$

where $J_h(q_f)$ is the hand Jacobian matrix defined as:

$$J_h(q_f) = \begin{bmatrix} B_{c_1}^T Ad_{g_{c_{f1}f_1}} J_{s_1 f_1}^{f_1} & 0 \\ 0 & B_{c_N}^T Ad_{g_{c_{fN}f_N}} J_{s_N f_N}^{f_N} \end{bmatrix}$$

This equation describes the grasp kinematics in terms of a set of ordinary differential equations.

(b) Grasp constraints of multi-fingered mobile manipulator

In this paper, the dexterous hands are mounted on the arms and then the velocities of the fingertips are related to those of the ends of the arms. Thus, a small change in the contact kinematics should be required. The contact kinematics is in the form:

$$J_B(q')\dot{q}_B' = G^T V_{Bo}^o \tag{34}$$

where $J_B(q')$ is the Jacobian matrix of the whole system defined as:

$$J_B(q') = \begin{bmatrix} B_{c_1}^T Ad_{g_{c_{f1}f_1}} J_{Bf_1}^{f_1} & 0 \\ 0 & B_{c_N}^T Ad_{g_{c_{fN}f_N}} J_{Bf_N}^{f_N} \end{bmatrix}$$

$q' = \begin{bmatrix} q_v^T & q_b^T & q_{f_1}^T & \cdots & q_{f_N}^T \end{bmatrix}^T$ has been defined in section 0; q_B' is the extension of vector q' and $q_B' = \begin{bmatrix} q_v^T & q_b^T & q_{f_1}^T & \cdots & q_v^T & q_b^T & q_{f_N}^T \end{bmatrix}$; V_{Bo}^o is the velocity of the object relative to the base frame in the object frame.

4.3 Contact Kinematics

In most of human and robotic hand tasks, rolling contact plays an important role in the mechanics of the manipulation. In this section we focus on the research of the manipulation which involves the rolling contacts by a set of fingers. An accurate modeling of the rolling phenomenon is fundamental for the research. We begin with a kinematic study of the case of one smooth finger rolling on a smooth object and extend the grasping formulation to the moving contacts. If the fingertip and the object shapes are completely known, the contact kinematics can be described by a suitable parameterization of the contact surfaces.

(a) Surface parameterizations [27]

Given an object in $\Re^3$, we describe the surface of the object using a local coordinate chart, C: $U \subset \Re^2 \to \Re^3$, as shown in Figure 9.

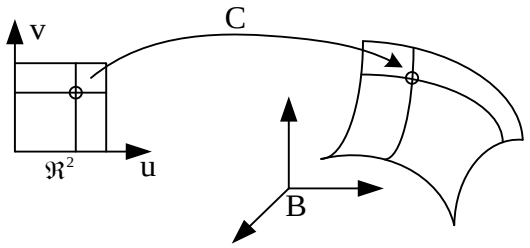

Figure 9: Surface chart for a two-dimensional object in $\Re^3$

Surface chart for a 2D object in $\Re^3$:

$$c(u,v) = [x(u,v), y(u,v), z(u,v)] \tag{35}$$

The map C takes a point $(u, v) \in \Re^2$ to a point $p \in \Re^3$ on the surface of the object, written in the object frame.

At any point on the object, we can define a tangent plane which consists of the space of all vectors which are tangent to the surface of the object at that point. The tangent plane is spanned by the vectors:

$$c_u = \frac{\partial c}{\partial u}, c_v = \frac{\partial c}{\partial v} \tag{36}$$

That is, any vector which is tangent to the surface at a point $c(u, v)$ may be expressed as a linear combination of the vectors c_u and c_v, evaluated at (u, v).

Given a parameterization, (M_p, K_p, T_p) are collectively referred to as the geometric parameters of the surface. These parameters describe the local geometry of the surface (metric tensor, curvature tensor, torsion) and play an important role in the kinematics of contact.

$$M_p = \begin{bmatrix} \| c_u \| & 0 \\ 0 & \| c_v \| \end{bmatrix}, K_p = \begin{bmatrix} \frac{c_u^T n_u}{\| c_u \|^2} & \frac{c_u^T n_v}{\| c_u \| \| c_v \|} \\ \frac{c_v^T n_u}{\| c_v \| \| c_u \|} & \frac{c_v^T n_v}{\| c_v \|^2} \end{bmatrix},$$
$$T_p = \begin{bmatrix} \frac{c_v^T c_{uu}}{\| c_u \|^2 \| c_v \|} & \frac{c_v^T c_{uv}}{\| c_u \| \| c_v \|^2} \end{bmatrix} \tag{37}$$

where $n_u = \frac{\partial n}{\partial u}, n_v = \frac{\partial n}{\partial v}, c_u = \frac{\partial c}{\partial u}, c_v = \frac{\partial c}{\partial v}$, while $c_{uu} = \frac{\partial^2 c}{\partial u^2}, c_{uv} = \frac{\partial^2 c}{\partial u \partial v}$, $n = N(u, v)$ is the unit normal at a point on the surface.

(b) Gauss Frame

The curvature, torsion, and metric tensors can also be computed in terms of a special coordinate frame called the normalized Gauss frame. If $c(u,v)$ is an orthogonal chart, we define the normalized Gauss frame as:

$$x = \frac{c_u}{\| c_u \|}, y = \frac{c_v}{\| c_v \|}, z = \frac{c_u \times c_v}{\| c_u \times c_v \|} \tag{38}$$

The normalized Gauss frame provides an orthonormal frame at each point on the surface.

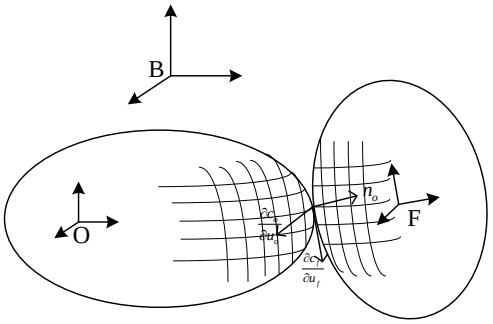

Figure 10: Motion of two objects in contact

Consider two objects with the surfaces S_o and S_f which are touching at a point, as shown in Figure 10. Let $p_o(t) \in S_o$ and $p_f(t) \in S_f$ be the positions at time t of the contact point relative to two body-fixed frames Σ_O and Σ_F, respectively. Let (c_o, U_o) and (c_f, U_f) be the charts for the two surfaces, and $\alpha_o = c_o^{-1}(p_o) \in U_o$ and $\alpha_f = c_f^{-1}(p_f) \in U_f$ be the local coordinates. Let ψ be the angle of contact, defined as the angle between the tangent vectors $\frac{\partial c_o}{\partial u_o}$ and $\frac{\partial c_f}{\partial u_f}$. We choose the sign of ψ so that a rotation of $\frac{\partial c_o}{\partial u_o}$ through an angle ψ around the outward normal of S_o aligns $\frac{\partial c_o}{\partial u_o}$ with $\frac{\partial c_f}{\partial u_f}$. Collecting the quantities which describe the contact, we obtain the contact coordinates $\begin{bmatrix} \alpha_f & \alpha_o & \psi \end{bmatrix}^T$ for S_f and S_o.

The contact kinematics allows the grasp matrix G and the hand Jacobian matrix J_h to be computed using the contact coordinates:

$$\kappa = \begin{bmatrix} \alpha_f & \alpha_o & \psi \end{bmatrix}^T = \begin{bmatrix} u_f & v_f & u_o & v_o & \psi \end{bmatrix}^T \tag{39}$$

In this work, it is assumed that the fingertips are semi-spheres and the object is a torus. Thus, the body-fixed frames Σ_F and Σ_O mentioned above are attached at the origin of the semi-sphere and the origin of the torus respectively. The geometric parameters of the sphere and the torus can be found in [28].

(c) Kinematic equations for rolling contact

We assume the pure rolling between the fingertips and the manipulated object. The motion of the contact coordinates, $\dot{\kappa} = \begin{bmatrix} \dot{\alpha}_f & \dot{\alpha}_o & \dot{\psi} \end{bmatrix}^T$, as a function of the relative motion is given by:

$$\begin{aligned} \dot{\alpha}_f &= M_f^{-1}(K_f + \tilde{K}_o)^{-1} \begin{bmatrix} -\omega_y \\ \omega_x \end{bmatrix} \\ \dot{\alpha}_o &= M_o^{-1} R_\psi (K_f + \tilde{K}_o)^{-1} \begin{bmatrix} -\omega_y \\ \omega_x \end{bmatrix} \\ \dot{\psi} &= T_f M_f \dot{\alpha}_f + T_o M_o \dot{\alpha}_o \end{aligned} \tag{40}$$

where $V_{c_o c_f}^{c_f} = \begin{bmatrix} v_x & v_y & v_z & \omega_x & \omega_y & \omega_z \end{bmatrix}^T$ has been defined in (30), $R_\psi = \begin{bmatrix} \cos\psi & -\sin\psi \\ -\sin\psi & -\cos\psi \end{bmatrix}$ and $\tilde{K}_o = R_\psi K_o R_\psi$.

Note that given the initial condition we can integrate the vector $\dot{\kappa}$ for each contact point and obtain the contact coordinates κ for each instant of time.

4.4 Constrained Dynamics of Dual-Hand Mobile Manipulator and Object System

The overall dynamics of a dual-hand mobile manipulator system manipulating an object is discussed in this section. In the previous section, we have analyzed the dynamics of the robot and the object which are all assumed free, i.e. neglecting the closure constraints. However, the physics of the robot

and the object as a whole system must be considered in a grasping task. To take into account the mutual relations and the wrenches exchanged between the fingers and the manipulated object we must slightly modify the dynamic equations.

First, recall the kinematic constraint equation in terms of $\dot{q}'$ which is the vector of the time derivative of the generalized coordinates q':

$$J_B \dot{q}_B' = G^T V_{Bo}^o \tag{41}$$

According to the nonholonomic constraints, for $\xi = \begin{bmatrix} v & \dot{q}_b & \dot{q}_f \end{bmatrix}^T$, there exists a full rank matrix $S'(q) \in \Re^{p' \times (p'-r)}$ that satisfies:

$$\dot{q}' = S' \xi \tag{42}$$

We have known that $\dot{q}_B'$ is the extension of $\dot{q}'$, thus there exists a matrix S_B' that satisfies:

$$\dot{q}_B' = S_B' \xi \tag{43}$$

The kinematic constraints become:

$$\begin{aligned} J_B S_B' \xi &= G^T V_{Bo}^o \\ J_B' \xi &= G^T V_{Bo}^o \end{aligned} \tag{44}$$

where $J_B' = J_B S_B'$.

From (44), the following kinematics can be derived:

$$J_B' \xi = G^T P^{-1} \dot{X}_o \tag{45}$$

We obtain the time derivative of (45):

$$\dot{J}_B' \xi + J_B' \dot{\xi} = \dot{G}^T P^{-1} \dot{X}_o + G^T \dot{P}^{-1} \dot{X}_o + G^T P^{-1} \ddot{X}_o \tag{46}$$

The matrix J_B' is not invertible due to the redundancy of the entire system. Equations (45) and (46) become:

$$\begin{aligned} \xi &= J_B^{\dagger} G^T P^{-1} \dot{X}_o + N\sigma \\ \dot{\xi} &= J_B^{\dagger} (\dot{G}^T P^{-1} \dot{X}_o + G^T \dot{P}^{-1} \dot{X}_o + G^T P^{-1} \ddot{X}_o - \dot{J}_B' (J_B^{\dagger} G^T P^{-1} \dot{X}_o + N\sigma)) \\ &\quad + N\sigma' \end{aligned} \tag{47}$$

where the symbol $\dagger$ denotes a weighted right pseudoinverse, $N = I - J_B^{\dagger} J_B'$ is a projector in the null space of the Jacobian matrix J_B', σ is a considered task function and σ' is another considered task function.

Assuming no friction, we should add a term $J_B'^T f_c$ to the complete dynamics of the mobile manipulator to take account of the forces exerted by the object on the fingertips:

$$\bar{M}' \dot{\xi} + \bar{C}' \xi + \bar{F}' = \bar{E}' \tau' - J_B'^T f_c \tag{48}$$

$$f_c = G^{\dagger} F_o + F_N \tag{49}$$

According to (48) and (49), the wrench applied to the object is equivalent to:

$$F_o = G J_B'^{\dagger T} (\bar{E}' \tau' - \bar{M}' \dot{\xi} - \bar{C}' \xi - \bar{F}') + GN' \sigma'' \tag{50}$$

where $N' = I - J_B'^{\dagger T} J_B'^T$ is a projector in the null space of the Jacobian matrix $J_B'^T$, and σ'' means the third considered task function.

If we replace ξ and $\dot{\xi}$ with (47), we obtain the wrench applied to the object as a format only with X_o, $\dot{X}_o$ and $\ddot{X}_o$:

$$\begin{aligned} F_o = G J_B'^{\dagger T} (&\bar{E}' \tau' - \bar{M}' (J_B^{\dagger} (\dot{G}^T P^{-1} \dot{X}_o + G^T \dot{P}^{-1} \dot{X}_o \\ &+ G^T P^{-1} \ddot{X}_o - \dot{J}_B' (J_B^{\dagger} G^T P^{-1} \dot{X}_o + N\sigma)) \\ &+ N\sigma') - \bar{C}' (J_B^{\dagger} G^T P^{-1} \dot{X}_o + N\sigma) - \bar{F}') + GN' \sigma'' \end{aligned} \tag{51}$$

Then we obtain the complete description of the dynamics of the whole robotic system composed of a mobile manipulator with multiple fingers and an object to be manipulated:

$$\tilde{M}\ddot{X}_o + \tilde{C}\dot{X}_o + \tilde{N} = GJ_B^{?T}\bar{E}'\tau' \tag{52}$$

where

$\tilde{M} = M_o + GJ_B^{?T}\bar{M}'J_B^{?}G^TP^{-1}$,

$\tilde{C} = C_o + GJ_B^{?T}\bar{M}'J_B^{?}(\dot{G}^TP^{-1} + G^T\dot{P}^{-1} - \dot{J}_B'J_B^{?}G^TP^{-1}) + GJ_B^{?T}\bar{C}'J_B^{?}G^TP^{-1}$,

$\tilde{N} = N_o + GJ_B^{?T}\bar{F}' - GJ_B^{?T}\bar{M}'J_B^{?}\dot{J}_B'N\sigma + GJ_B^{?T}\bar{M}'N\sigma' + GJ_B^{?T}\bar{C}'N\sigma - GN'\sigma''$.

5. Computed Torque Control for Object Manipulation with Mobile Manipulator

In this section, an object manipulation method is proposed by the computed torque method based on the accurate model for the robot-object system.

Substituting (47) and (49) into the dynamic equitation of the complete dynamic model which considers the external wrench:

$$\begin{aligned}&\bar{M}'(J_B^{?}(\dot{G}^TP^{-1}\dot{X}_o + G^T\dot{P}^{-1}\dot{X}_o + G^TP^{-1}\ddot{X}_o - \dot{J}_B'(J_B^{?}G^TP^{-1}\dot{X}_o + N\sigma))\\&+N\sigma') + \bar{C}'(J_B^{?}G^TP^{-1}\dot{X}_o + N\sigma) + \bar{F}'\\&= \bar{E}'\tau' - J_B^{'T}(G^{?}(M_o\ddot{X}_o + C_o\dot{X}_o + N_o) + F_N)\end{aligned} \tag{53}$$

And rearranging it we have:

$$\begin{aligned}&(\bar{M}'J_B^{?}G^TP^{-1} + J_B^{'T}G^{?}M_o)\ddot{X}_o\\&= \bar{E}'\tau' - J_B^{'T}(G^{?}(C_o\dot{X}_o + N_o) + F_N) - \bar{F}' - \bar{C}'(J_B^{?}G^TP^{-1}\dot{X}_o + N\sigma)\\&-\bar{M}'(J_B^{?}(\dot{G}^TP^{-1}\dot{X}_o + G^T\dot{P}^{-1}\dot{X}_o - \dot{J}_B'(J_B^{?}G^TP^{-1}\dot{X}_o + N\sigma)) + N\sigma')\end{aligned} \tag{54}$$

We adopt the following method to track the desired trajectory $X_d(t)$:

$$\begin{aligned}\bar{E}'\tau' &= J_B^{'T}(G^{?}(C_o\dot{X}_o + N_o) + F_N) + \bar{F}' + \bar{C}'(J_B^{?}G^TP^{-1}\dot{X}_o + N\sigma)\\&+\bar{M}'(J_B^{?}(\dot{G}^TP^{-1}\dot{X}_o + G^T\dot{P}^{-1}\dot{X}_o - \dot{J}_B'(J_B^{?}G^TP^{-1}\dot{X}_o + N\sigma)) + N\sigma')\\&+(\bar{M}'J_B^{?}G^TP^{-1} + J_B^{'T}G^{?}M_o)(\ddot{X}_d + K_v\dot{E}_{X_o} + K_pE_{X_o})\end{aligned} \tag{55}$$

where $\dot{E}_{X_o} = \dot{X}_d - \dot{X}_o$ and $E_{X_o} = X_d - X_o$, respectively, are the errors of the velocity and the trajectory of the object while Kv and Kp are diagonal matrices whose values are, respectively, the derivative and the proportional coefficients.

In this paper, LMI is used to optimize the grasping forces and then the internal force F_N in the above equation can be obtained.

Proof: We replace τ' with (55) in (54) and obtain:

$$\begin{aligned}\bar{M}'J_B^{?}G^TP^{-1}\ddot{X}_o &= (\bar{M}'J_B^{?}G^TP^{-1} + J_B^{'T}G^{?}M_o)(\ddot{X}_d + K_v\dot{E}_{X_o} + K_pE_{X_o})\\&- J_B^{'T}G^{?}M_o\ddot{X}_o\end{aligned} \tag{56}$$

Then the error dynamics is as following:

$$\ddot{E}_{X_o} + K_v\dot{E}_{X_o} + K_pE_{X_o} = 0 \tag{57}$$

The uniform ultimate boundedness of the tracking error can be proved from (57).

6. Simulation Results

This section gives some simulation results of object manipulation with the robot equipped with a pair of dexterous hands. For simulation, the robot with the dexterous hands is developed using MATLAB (Figure 11) which has the same structure as the real one. And all the links are simplified and are represented with columns. The initial configuration of the center of mass of the object

is $X_{oinit} = [x_o \quad y_o \quad z_o \quad \alpha_o \quad \beta_o \quad \gamma_o]^T$, where the first three components represent the position of the object relative to the base frame, and the last three ones describe the orientation of the object.

Assume that a precision grasp is applied to the object. The task is designed as follows: starting from the initial configuration, the assistant robot grasps an object from the right hand side while making the left hand-arm system keep the initial configuration; given an initial configuration X_{oinit} , the object moves along a desired trajectory described by following function $X_o = [x_o + t \quad y_o \quad z_o \quad \alpha_o \quad \beta_o \quad \gamma_o]^T$.

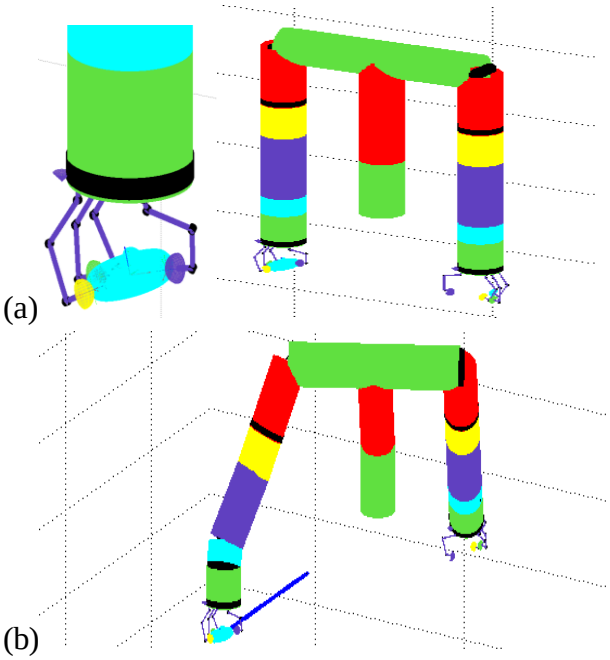

(a) (b)

Figure 11: Object manipulation by mobile manipulator (a) Initial configuration of mobile manipulator and object system (b) Final configuration of mobile manipulator and object system

Figure 11 and Figure 12 show the numerical simulation results of object manipulation by the complete mobile manipulator. Figure 11(a) and Figure 11(b) illustrate the initial and final configurations of the composite system during one run of the grasping algorithm. From Figure 11(b), it is observed that the robotic system can successfully manipulate the object without slippage, and at the same time the joints of left hand-arm system keep stationary.

The object can well follow the desired trajectory as illustrated in Figure 12(a) which shows the motion in the x direction. Figure 12(b) shows the motions along the y and z directions. The Euler angles which represent the orientation are also shown in this figure. In Figure 12(c), threes curves depict the motion of the mobile platform which assists the hand to achieve the task. Figure 12(d), (e) and (f) show the joint torques of the fingers, the wheels, dual arms and the waist calculated by the algorithm, respectively. The simulation results validate the usefulness of the proposed control method.

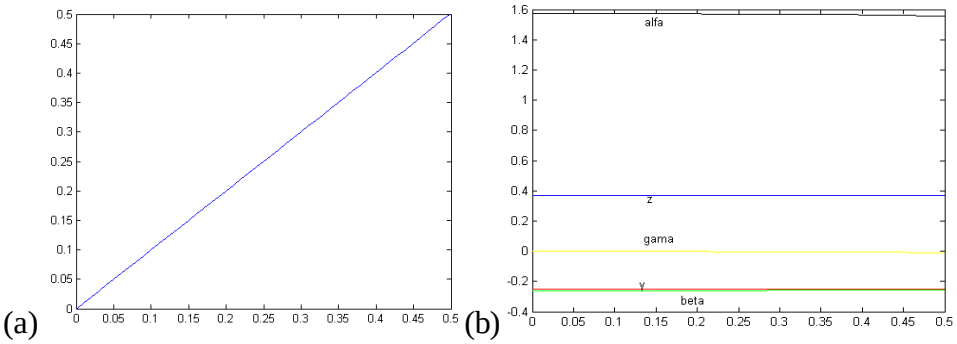

(a) (b)

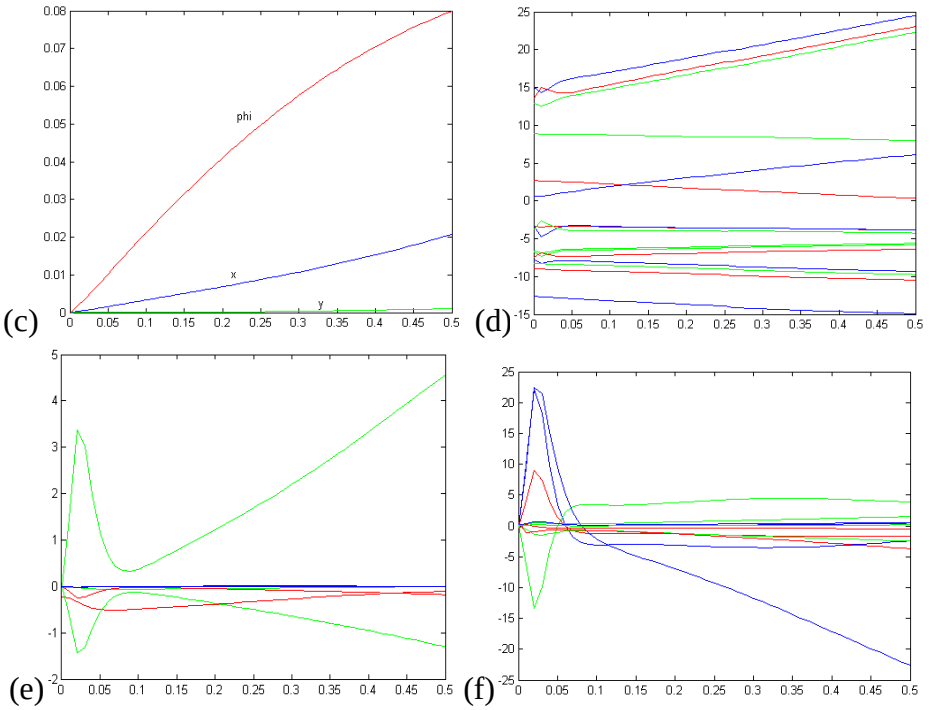

Figure 12: Simulation results (a) The motion in x-direction (b) The motions in y, z- directions and the orientation change (c) Motions of mobile base (d) Joint torques of fingers (e) Joint torques of left arm (f) Joint torques of wheels, waist and right arm

The optimal normal and tangential forces at all contact points are described in Figure 13. It can be seen that the contact forces all satisfy the friction cone constraints.

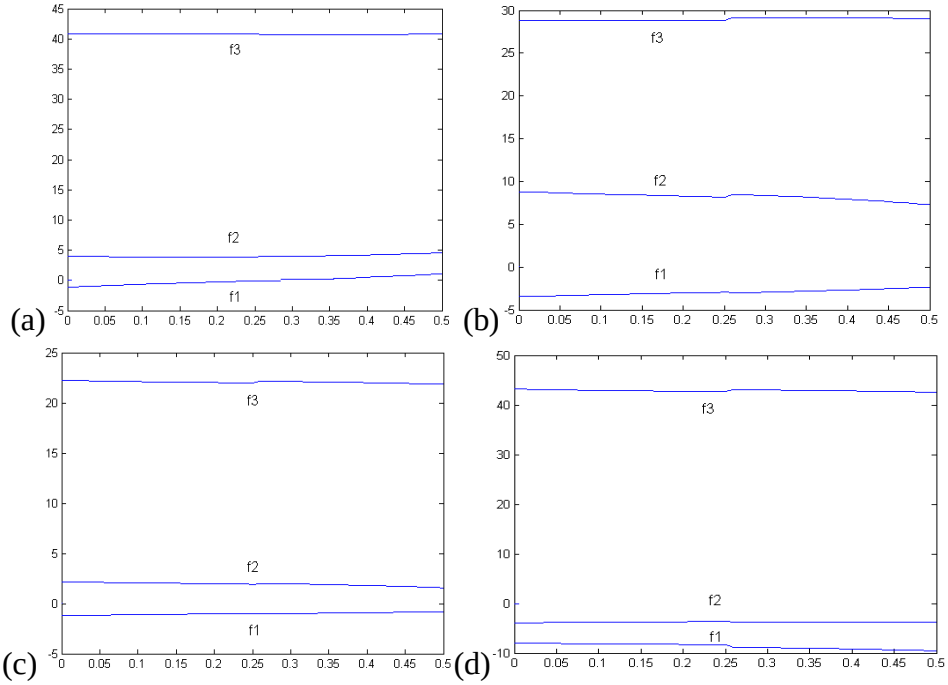

Figure 13: Magnitude of contact forces (a) Contact forces of finger 1 (b) Contact forces of finger 2 (a) Contact forces of finger 3 (b) Contact forces of finger 4

7. Conclusion

The paper sets up the complete kinematic and dynamic models for the personal assistant robot and the constrained models of the robot–object system are also given. The kinematics is established by using the MDH method and the dynamics is analyzed by Lagrange's theorem. We have also presented an efficient control method for object manipulation. This control method is based on the precise constrained dynamic model which has been well developed. The object manipulation is realized in MATLAB environment. Simulation results show that the proposed method for object manipulation is effective. This method can ensure firm grip, avoid slippage and well track a given motion imposed to the object.

References

[1] Y. Yamamoto and X. Yun, "A modular approach to dynamic modeling of a class of mobile manipulators," International Journal of Robotics and Automation, vol. 12, no. 2, pp. 41-48, 1997.
[2] Q. Yu, I. M. Chen, "A general approach to the dynamics of nonholonomic mobile manipulator systems," ASME J. Dyn. Syst. Meas. Control 124, 512–521 (2002).
[3] H. G. Tanner and K. J. Kyriakopoulos, "Mobile manipulator modeling with Kane's approach," Robotica, vol. 19, pp. 675-690, 2001.
[4] L. Sheng, A. A. Goldenberg, "Neural-network control of mobile manipulators," IEEE Transactions on Neural Networks, vol. 12, no. 5, pp. 1121-1133, 2001.
[5] Y. Yamamoto and X. Yun, "Unified analysis on mobility and manipulability of mobile manipulators," in Proc. IEEE International Conference on Robotics and Automation, pp. 1200–1206, 1999.
[6] Y. Yamamoto, X. Yun, "Coordinating locomotion and manipulation of a mobile manipulator," in Proc. the 31th Conference on Decision and Control, Tucson, AZ, pp. 2643-2648, Dec.1992.
[7] T. Okada, Computer control of multijointed finger system for precise object handling, International Trends in Manufacturing Technology-Robot Grippers, 1986.
[8] K. S. Salisbury and B. Roth, Kinematics and force analysis of articulated mechanical hands, Journal of Mechanims, Transmissions and Actuation in Design, 1983.
[9] S. C. Jacobsen et al., Design of the utah/mit dexterous hand, Proc. IEEE International Conference on Robotics and Automation.
[10] C. S. Lovchik and M. A. Diftler, The robonaut hand: a dexterous robot hand for space, Proc. IEEE International Conference on Robotics and Automation, 1999.
[11] J. Butterfass, M. Grebenstein, H. Liu, and G. Hirzinger, Dlr-hand II: Next generation of a dextrous robot hand, Proc. IEEE International Conference on Robotics and Automation.
[12] H. Kawasaki, H. Shimomura, and Y. Shimizu, Educational-industrial complex development of an anthropomorphic robot hand 'gifu hand', Advanced Robotics, 15, no.3, 2001.
[13] G. Berselli, G. Borghesan, M. Brandi, C. Melchiorri, C. Natale, G. Palli, S. Pirozzi, and G. Vassura, Integrated mechatronic design for a new generation of robotic hands, 8th IFAC International Symposium on Robot Control, 2009.
[14] T. Asfour, K. Regenstein, and P. Azad et al, "ARMAR-III: An integrated humanoid platform for sensory-motor control," in Proc. 6th IEEE-RAS International Conference on Humanoid Robots, 2006.
[15] Meka webpage: http://mekabot.com/products/m1- mobile-manipulator/.
[16] Jacques Denavit and Richard S. Hartenberg, "A kinematic notation for lower-pair mechanisms based on matrices," ASME Journal of Applied Mechanics, pages 215–221, June 1955.
[17] Mark W. Spong and M. Vidyasagar. Robot Dynamics and Control. John Wiley & Sons, Ltd, New York, 1989.
[18] J. J. Craig, Introduction to Robotics, Addison Wesley, second ed., 1989.
[19] J. Chung, S. Velinsky, "Robust control of a mobile manipulator-dynamic modelling approach," Proceedings of the American Control Conference, pp. 2435-2439, San Diego, California, USA, 1999.

[20] Q. Yu, I. Chen, "A general approach to the dynamics of nonholonomic mobile manipulator systems," ASME Trans. of Dynamic Systems, Measurement, and Control, Vol. 124, No. 4, pp. 512-521, 2002.
[21] H. Tanner, K. Kyriakopoulos, "Mobile manipulator modelling with Kane's approach," Robotica, Vol. 19, pp. 675-690, 2001.
[22] W. Jingguo, L. Yangmin, "Dynamic Modeling of a Mobile Humanoid Robot," In IEEE Int. Conf. on Robotics and Biomimetics, Bangkok, Thailand, pp. 639-644, 2009.
[23] L. Han, J. C. Trinkle, and Z. X. Li, "Grasp analysis as linear matrix inequality problems," IEEE Trans. Robotics and Automation, vol. 16, pp. 663–674, Dec. 2000.
[24] M. Buss, H. Hashimoto, and J. B. Moore, "Dextrous hand grasping force optimization," IEEE Trans. Robotics and Automation, vol. 12, pp. 406–417, June 1996.
[25] Y. Yamamoto, X. Yun, "Coordinating locomotion and manipulation of a mobile manipulator," in Proc. the 31th Conference on Decision and Control, Tucson, AZ, pp. 2643-2648, Dec.1992.
[26] F. L. Lewis and S. Jagannathan, Neural network control of robot manipulators and nonlinear systems, London: Taylor & Francis, 1999.
[27] R. M. Murray, Z. X. Li and S. S. Sastry, A Mathematical Introduction to Robotic Manipulation, CRC Press, 2000 Corporate Blvd., N.W., Boca Raton, Florida 33431, ISBN 0-8493-7981-4, 1994.
[28] Antonino Lo Biondo, Giulio Mancuso, Analisi e controllo manipolazione robotica (Analysis and Control of Robotic Manipulation), Technical Report, University of Pisa.